JOURNAL OF CRITICAL REVIEWS

ISSN- 2394-5125 VOL 7, ISSUE 05, 2020

Isothermal and kinetics of biosportion capacity of crystal violet dye by using Red algae *Gelidium pusillum*

Satyaprasad Y, Asha Immanuel Raju Ch, Jaganada Rao P*

Research scholar, Department of Chemical Engineering, College of Engineering, Andhra University, Vishakhapatnam, Andhrapradesh, India.

Assistant Professor, Department of Chemical Engineering, College of Engineering, Andhra University, Vishakhapatnam, Andhrapradesh, India.

Professor, Department of Chemical Engineering, College of Engineering, Andhra University, Vishakhapatnam, Andhrapradesh, India.

Corresponding author

Professor,

Department of Chemical Engineering, College of Engineering, Andhra University, Vishakhapatnam, Andhra Pradesh, India, Contact number:+919849471777

Email.id:pjencon@gmail.com

Abstract

Biosorption is a process by using different biological absorbents we are removing the chemical contaminants such as toxic metals and dyes from industrial effluents. In the current study we are analysed FIIR and XRD for confirming the functional groups and crystal nature of *G pusillum* and study the isothermal, thermodynamics and kinetics properties of adsorption by using standard procedures. The maximum adsorption of CV dye (90.23709 %) onto *G. pusillum* is observed from the current investigation also reveals the endothermic nature of sorption as ΔH is positive (14.7433 J/mole), irreversible nature of sorption as ΔS is positive (13.0993 J/mole.K) and spontaneity of sorption as indicated by negative ΔG (–1105.35 J/mole).

Keywords: Biosorption, *G pusillum*, FIIR, XRD, Thermodynamics, Kinetics.

1. Introduction

Wastewaters from textile, paper, and colouring industries are continuously polluted by dyes and effects ecosystem of life, the dye pollution is a harmful and significant problem faced by many developed and developing countries [1]. Even at low concentrations dyes affect aquatic and terrestrial system, in textile and paper industries dyes such as methylene blue, saffarine, crystal violet, congo red and phenol red are directly released in to the aquatic system [2] These dyes are unable to decomposed by physical, chemical and microbial process, which are most obstinate compound which are carcinogenic, mutagenic, triggers allergic reactions in human [3].Many methods such as activated carbon adsorption, chemical oxidation, coagulation, ultra-filtration, electrochemical etc. have been developed for treating dye-containing wastewaters [4]. All these methods having their own disadvantages for removing of contaminated dyes from both industrial and domestic waste, therefore, many scientific approaches have been made to find best and cheaper methods for removal of dyes

ISSN- 2394-5125 VOL 7, ISSUE 05, 2020

[5].Different materials such as low-cost sorbents such as peat, perlite , sawdust [6], etc. have been utilized for dye removal.

Among all the wastewater treatments, the adsorption process has been recognized to be an effective and economical procedure for the removal of dyes from industrial effluent [7]. Three methods such as biodegradation, bioaccumulation and biosorption have been continually used for the dye removal process. On the other hand, biosorption process has also been commonly used for the removal of dyes as well as heavy metal and organic pollution. Bisoprtion is a bioremediation process in which by using biological materials such microflora, plant materials, animal materials and sea products removes the chemical pollutants such as heavy metals, toxins and dyes [8]. Isotherm explains adsorption capacity of adsorbate, on adsorbents such as stronger or weaker interactions, adsorbate capacity on adsorbents depends on pressure, concentration at constant temperature[9].Biosorption kinetics shown, the rate adsorbate (Dyes, heavy metals, pollutants, etc.,) binding on to the surface of adsorbents (biological materials), and explains about biosorption process and rate constant[10]. The thermodynamics of biosorption deals with, capacity of biosoprtion, endothermic nature of biosorption, and affinity of biosorbents. Due to some limitations in biological adsorbents, scientists are forced develop novel biological adsorbents from natural sources hence the current study was focused on isolation of biological (Red Algae) source from marine water for development of natural biological adsorbents *gelidium pusillum*. The functional groups involved in biosorption process were evaluated by FTIR and crystal nature of prepared biological adsorbents XRD.

2. Methodology

2.1 Preparation of the bisorbents[11]

Gelidium pusillum were gathered from Tenneti Park, Jodugullapalem sea shore in Visakhapatnam city, Andhra Pradesh, India. After through washing with distilled water, biosorbents were sun dried until they became fresh, cut into little pieces, powdered and sieved. In the current review, 53, 75, 105, 125 and 152 µm size powders were utilized as biosorbents with no other pretreatments.

2.2 Characterization of biosorbents

2.2.1 FTIR studies [12]

Biosorbents were portrayed by FTIR spectrometry utilizing Spectrum GX of Perkin Elmer, USA spectrophotometer from 400 to 4000 cm^{-1} with a goal of 1 cm-1 utilizing 4 outputs with foundation deduction. In the wake of getting the spectra, the pinnacles were distinguished by contrasting and the spectra detailed in writing.

2.2.2 X-ray diffraction analysis [13]

The X-Ray Diffractograms (XRD) of the powder tests are taken utilizing a Rigaku Ultima model IV. The diffracted X-beam forces are recorded as an element of 2α by utilizing copper target (Cu-Kα radiation with frequency, α= 1.5492 Å) at a sweep speed of 20/min. XRD designs are recorded from 3 to 900. Various periods of the examples are to be distinguished by contrasting and a bunch of'd' values and the comparing forces with the guidelines from the ICDD (International Center for Diffraction Data) documents.

3. Results and Discussion

3.1. Fourier Transform Infra-Red Spectroscopy (FTIR)

ISSN- 2394-5125 VOL 7, ISSUE 05, 2020

3.1.1 FTIR spectrum of untreated CV dye[14]

FTIR measurements presented in below figure 1(a) shows the presence of C-I stretch at a band of 399.2267 cm^{-1}. The skeletal C-C vibrations are observed at a broad band of 786.87366 cm^{-1}. The band at 1095.45157 cm^{-1} is due to the carbohydrate vibrations represented by glucose, fructose and glycogen. The 1378.95752 cm^{-1} indicates $–CH_2$ bending vibrations. The presence of Alkyl C-H stretch is indicated by the bands at 1863.03911cm^{-1}, 2092.54393 cm^{-1}, 2289.26234 cm^{-1}, 2493.69521 cm^{-1}, 2673.05611 cm^{-1}. The band at 3479.2159 cm^{-1} denotes the presence of O-H stretching modes.

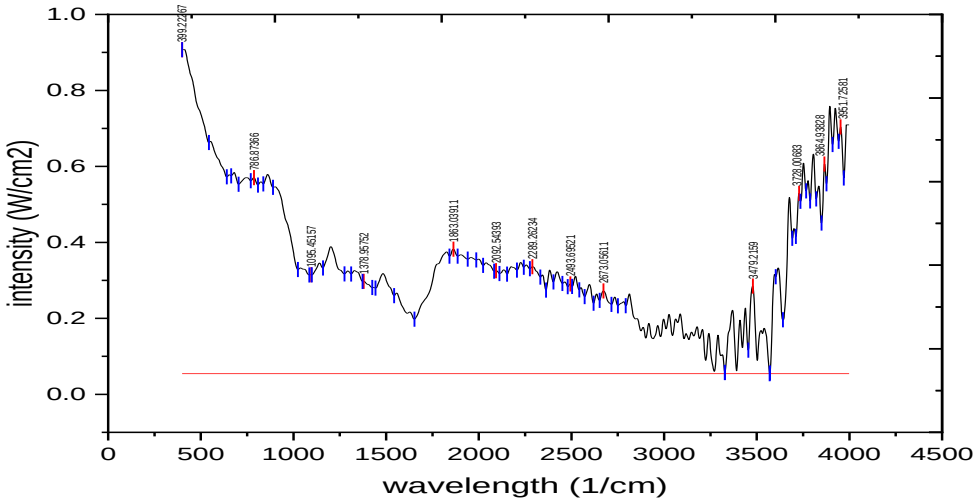

Fig-1 (a) FTIR spectrum of CV dye untreated *G. Pusillum*

3.1.2 FTIR spectrum of CV dye treated with *G. pusillum*

FTIR measurements presented in below figure1 (b) shows the presence of C-I stretch at band of 420.4374 cm^{-1}. The band at 547.72578 cm^{-1} is due to C-Br stretch. The cis = C-H out of plane bending is observed at a band of 771.44477 cm^{-1}. The band at 929.59094 cm^{-1} is shows the cyclohexane vibrations. The band at 1270.95525 cm^{-1} is due to the SO_3 stretching. The band at 1396.31503 cm^{-1} indicates S=O and C-S-O bends from ester sulfonate. The band at 1508.17452 cm^{-1} is suggests the presence of H-C-H interactions. . The presence of Alkyl C-H stretch is indicated by the bands at 1772.39435 cm^{-1}, 1890.03966 cm^{-1}, 2017.32806 cm^{-1}, 2167.75979 cm^{-1}, 2343.26348 cm^{-1}, 2491.76659 cm^{-1}, 2653.77 cm^{-1}. The band at 2869.77453 cm^{-1} is controlled by the anti symmetric and symmetric C-H stretches. The band at 3618.07595 cm^{-1} is indicated by O-H stretching modes.

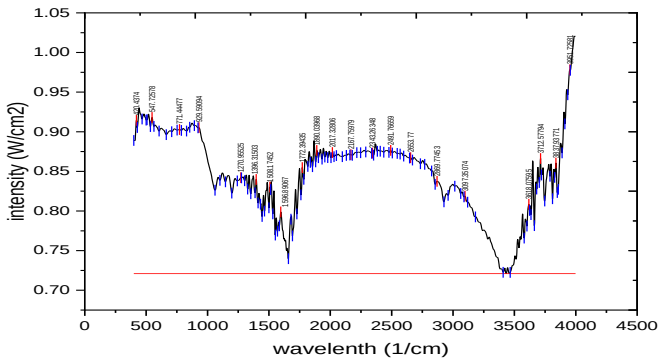

Fig. 1 (b) FTIR spectrum of CV dye treated *G pusillum*

ISSN- 2394-5125 VOL 7, ISSUE 05, 2020

3.2. X-Ray Diffraction studies.

3.2.1. XRD for CV dye untreated with *G. pusillum* [15]

XRD designs for untreated powder [Figs.2 (a) and 2(b)] show great crystallinity, more indistinct nature and increment in surface region and porosity The peaks at 2theta values of 10.12, 10.40, 10.84 corroborate the presence of heptasodiumhexaniobate, Ge9 K4 (NH3)9, Os7 (CO)20 (S)2 with corresponding d values are 8.7337, 8.4991 and 8.1551 respectively.

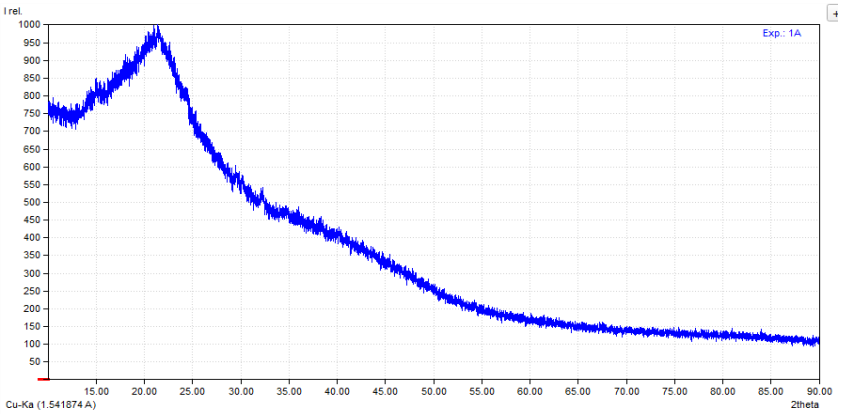

Fig .2(a) XRD pattern of CV dye untreated *G.Pusillum*

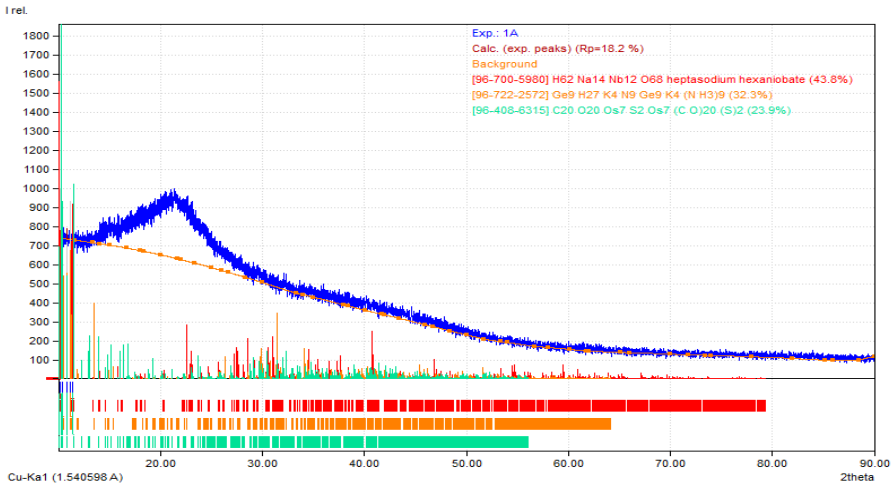

Fig. 2 (b) XRD pattern of CV dye untreated *G. pusillum* with matching compounds

3.2.2 XRD for CV dye treated with *G. pusillum* [16]

XRD designs for treated powder [Figs.2(c) and 2 (d)] show great crystallinity, more indistinct nature and increment in surface region and porosity. The tops at 2θ estimations of 0.7765, 0.6899, 0.6084, 0.5983 and 0.5397 support the nearness of Fe39Sb9Se4, AS14Cs4Zn, O9P3Y, F7RuXe and Cl2H12P4Ru. Their relating d-values are 3.9371, 3.7334, 3.4874, 3.4391 and 3.6449. The progressions in 2α values and compounds for when show that biosorption has happened.

ISSN- 2394-5125 VOL 7, ISSUE 05, 2020

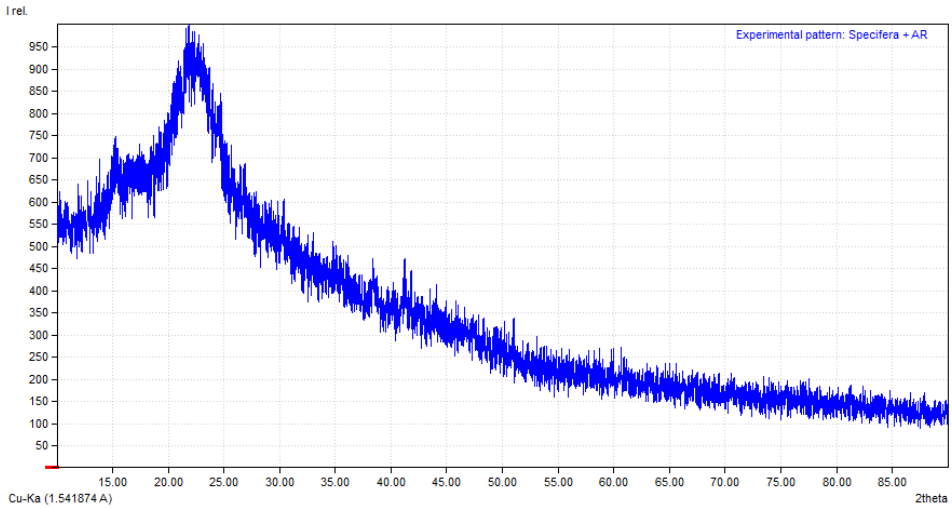

Fig. 2 (c) XRD pattern of CV dye treated *G. pusillum*

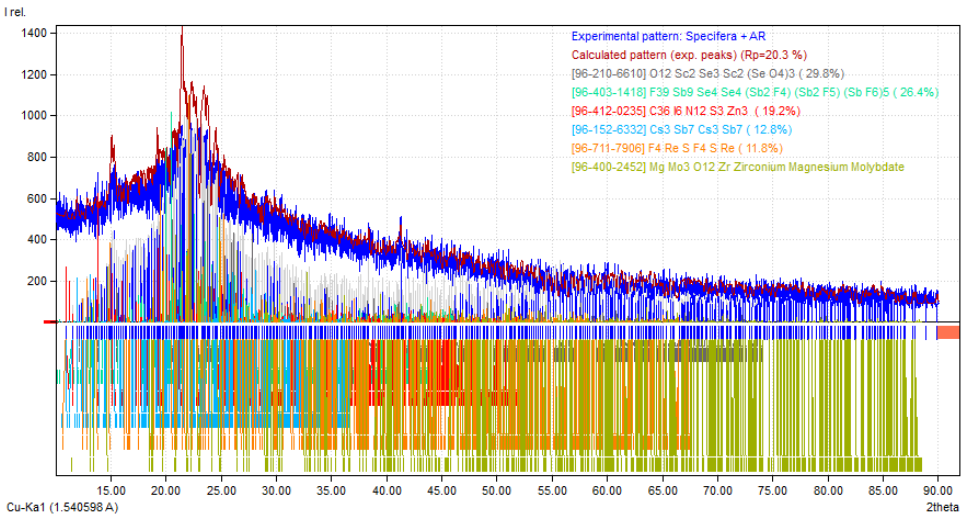

Fig. 2 (d) XRD pattern of CV dye treated *G. pusillum* powder with matching compounds

4. Isotherms

4.1. Langmuir isotherm [17]

Langmuir isotherm is the most broadly utilized straightforward two-boundary condition. This basic isotherm depends on following suppositions:

• Adsorbate is synthetically adsorbed at a fixed number of all around characterized locales

•Each site can hold just a single adscience and nature sorbate animal types

•All destinations are vivaciously proportional

•There are no connections between the adsorbate species

The Langmuir relationship is hyperbolic and the condition is:

$qe/qm = KLCe/(1+KLCe)$ - (1)

The above condition can be revamped as

$(Ce/qe) = 1/(KLqm) + Ce/qm$ - (2)

ISSN- 2394-5125 VOL 7, ISSUE 05, 2020

From the plots between (Ce/qe) and Ce, the incline {1/(KLqm)} and the capture (1/qm) can be determined. Further investigation of Langmuir condition can be made based on division factor [RL =1/(1+KLCe)].

0< RL<1 shows positive adsorption

RL|>|1 shows horrible adsorption

RL = 1 shows direct adsorption

RL = 0 shows powerful adsorption

Langmuir isotherm is drawn between Ce/qe and Ce in fig.3, for the current information. The subsequent condition is

(Ce/qe) = 0.055 Ce + 6.370 - (.3)

The (connection coefficient of 0.983) affirms solid official of CV dye particles to the outside of *G. pusillum*

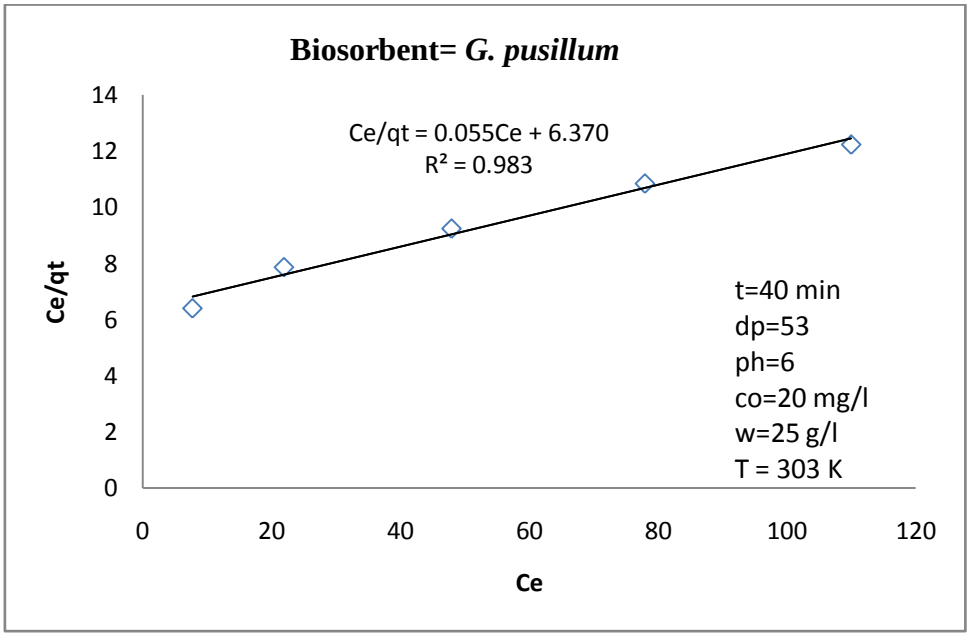

Fig. 3 Langmuir isotherm for biosorption

4.2. Freundlich isotherm [17]

Freundlich introduced an observational adsorption isotherm condition that can be applied incase of low and middle of the road fixation ranges. The Freundlich isotherm is given by qe = Kf Cen - (4)

Where Kf, mg/g speaks to the adsorption limit at dye harmony fixation and n speaks to the level of reliance of adsorption.

Taking LN on the two sides, we get ln qe = ln Kf+ n ln Ce - (.5)

Freundlich isotherm is drawn between ln Ce and ln qe in fig.4, brought about the accompanying condition ln qe = 0.76 ln Ce–1.337 - (6)

The condition has a relationship coefficient of 0.998

. The 'n' estimation of 0.7334 shows ideal biosorption satisfying the condition of 0<n<1.

ISSN- 2394-5125 VOL 7, ISSUE 05, 2020

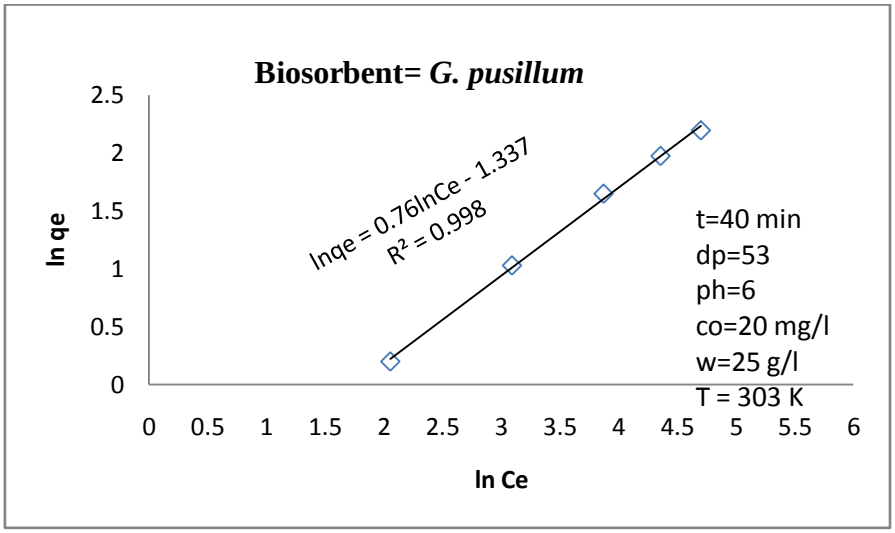

Fig.4 Freundlich isotherm for biosorption

4 .3 Temkin isotherms: **[17]**

Temkin and Pyzhev isotherm condition depicts the conduct of numerous adsorption frameworks on heterogeneous surface and depends on the condition:

qe= RT ln(ATCe)/bT - (7)

The direct type of Temkin isotherm is qe= (RT/bT) ln(AT) + (RT/bT) ln(Ce) - (.8)

AT= exp [b (0) x b (1)/RT] Slope, b (1) = RT/bT Intercept, b (0) = (RT/bT) ln (AT)

Plot among qe and ln Ce is appeared in fig. 5. The condition for CV dye biosorption is qe= 2.903 ln Ce – 5.409 - (.9)

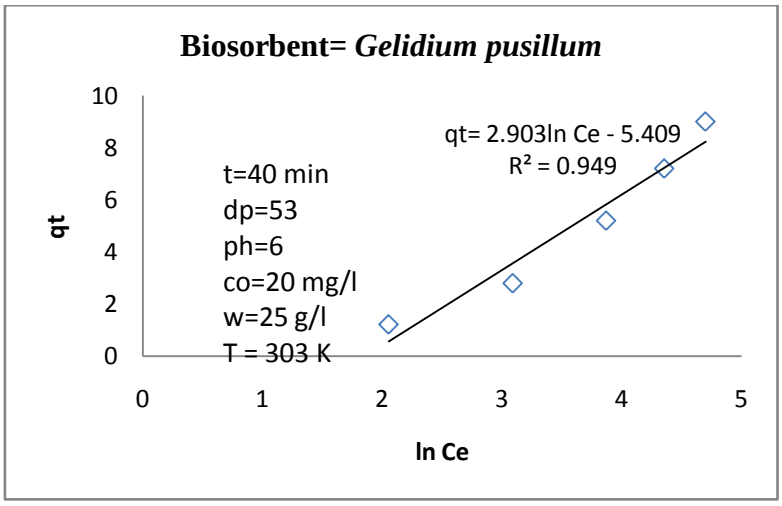

Fig.5 Temkin isotherm for biosorption

The isotherm constants are assembled in table-1. It is discovered that biosorption information are all around spoke to by Langmuir isotherm (R^2=0.983), Freundlich isotherms (R^2=0.998) and Temkin (R^2=0.949)

Table 1 Isotherm constants

Langmuir isotherm	Freundlich isotherm	Temkin isotherm
q_m = 18.18 mg/g	K_f = 0.2626mg/g	AT= 0.1551 L/mg
K_L = 0.008634	n = 0.76	BT = 867.772
R^2 = 0.983	R^2 = 0.998	R^2 = 0.949

ISSN- 2394-5125 VOL 7, ISSUE 05, 2020

5. Kinetics

5.1 Lagergren first order

Lagergren plot and pseudo second request energy plot for biosorption of CV dye are attracted figs. 6 and 7. Table-2 sums up the rate steady qualities for first and second request rate conditions [18]. It is noticed that both first and second request rate conditions clarify the biosorption collaborations sufficiently.

log (qe-qt) = – 0.028 t + 0.0174, R^2=0.929

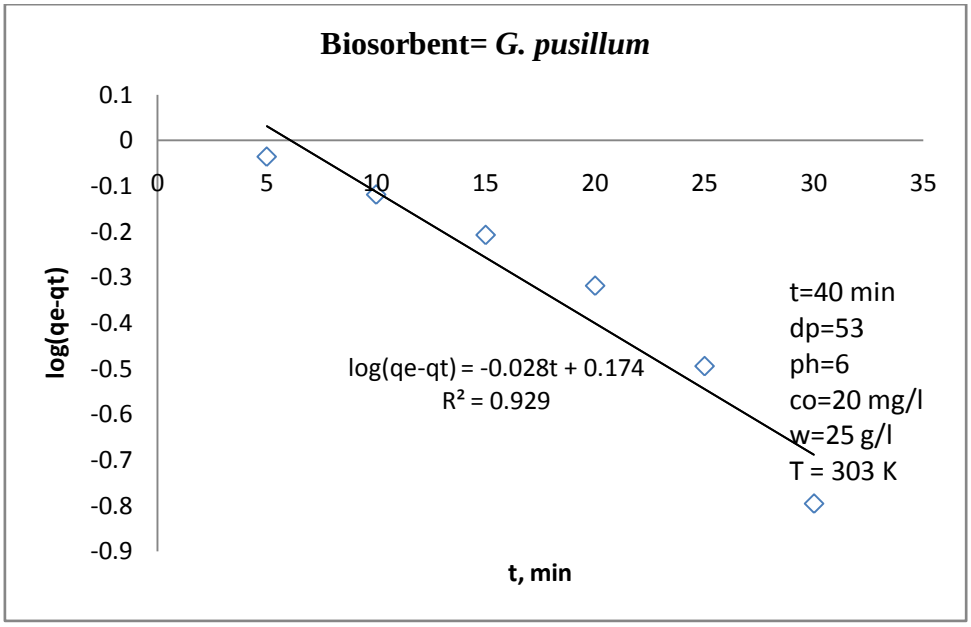

Fig.6 .First order kinetics for biosorption

5.2 Pseudo second order

Second request rate conditions clarify the biosorption cooperations agreeably **[**19, 20**]**. The rate consistent qualities for second request rate conditions

t/qt = 0.245 t + 25.13, R^2=0.806

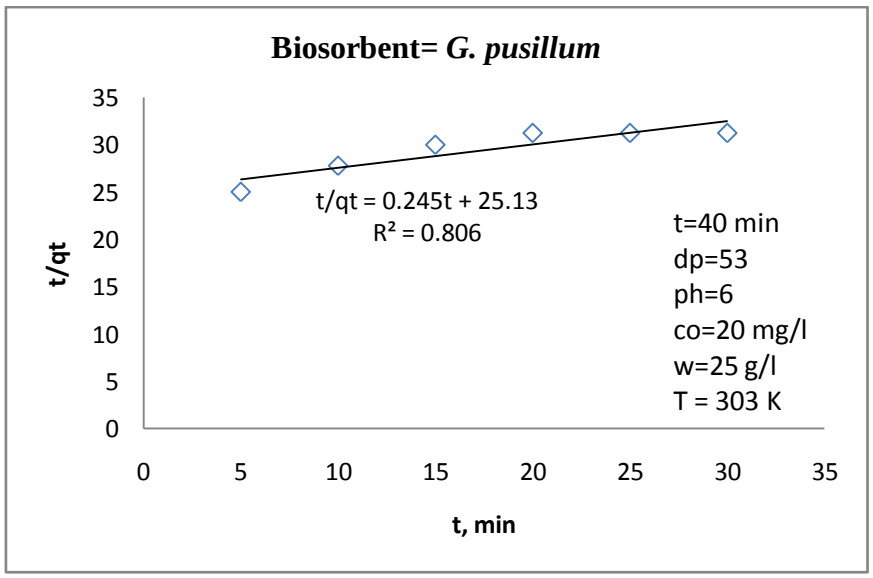

Fig.7 .Second order Kinetics for biosorption

ISSN- 2394-5125 VOL 7, ISSUE 05, 2020

Table 2 Equations and rate constants

Order	Equation	Rate constant	R^2
Lagergren first order	$\log (q_e-q_t) = -0.028\ t + 0.0174$	0.0644 min^{-1}	0.929
Pseudo second order	$t/q_t = 0.245\ t + 25.13$	0.0023 g/ (mg-min)	0.806

6. Thermodynamics

Van't Hoff's plot is attracted fig.8. From the information, Gibbs free vitality change (ΔG) is determined to be – 1105.35 J/mol for biosorption of CV dye. The negative ΔGvalue demonstrates thermodynamically possible and unconstrained nature of biosorption. The ΔH boundary is 14.7433 kJ/mol.K. The negative ΔH demonstrates the endothermic idea of biosorption. ΔS boundary is discovered to be 13.0993 J/mol K for CV dye biosorption [21, 22]. The positive ΔSvalue recommends an expansion in the irregularity at the strong/arrangement interface during biosorption.

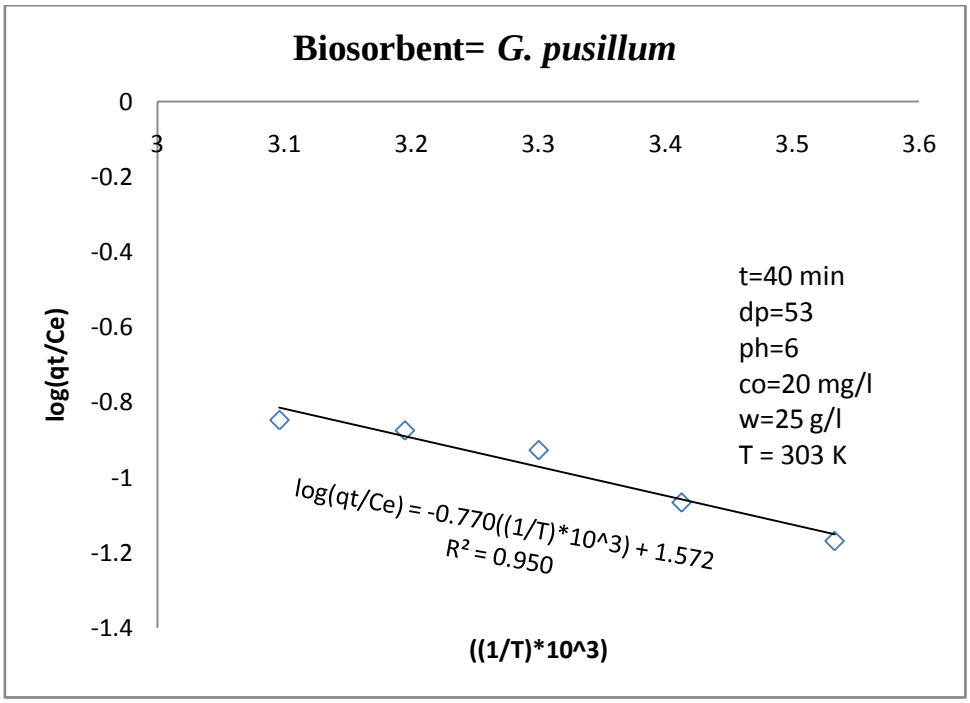

Fig.8.Vant Hoff's plot for biosorption

7. Optimization using Response Surface Methodology (RSM):

7.1 Optimization using CCD

The boundaries that have more prominent impact over the reaction are to be recognized to locate the ideal condition for the biosorption of CV dye. The quadratic model is utilized in the current investigation, to relate four autonomous factors and rate biosorption of CV dye. The relapse condition for is % biosorption of CV dye is capacity of pH (X1), Co (X2), w (X3) and T (X4) [23,24].

The varieties in the relating coded estimations of four boundaries and reaction are introduced in table-.3 and their respective results were shown in table-4.

ISSN- 2394-5125 VOL 7, ISSUE 05, 2020

Table-.3 Levels of different process variables in coded and un-coded form for % biosorption of CV dye using *G. pusillum*

Variable	Name	Range and levels				
		-2	-1	0	1	2
X_1	pH of aqueous solution	4	5	6	7	8
X_2	Initial concentration, C_o, mg/L	10	15	20	25	30
X_3	Biosorbent dosage, w, g/L	15	20	25	30	35
X_4	Temperature, T, K	283	293	303	313	323

The accompanying condition speaks to different relapse investigation of the test information for the biosorption of CV dye:

$$Y = -2341.18 + 47.94X_1 + 1.94X_2 + 0.84X_3 + 9.92X_4 - 6.75X_1^2 - 0.08X_2^2 - 0.08X_3^2 - 0.02X_4^2 + 0.06X_1X_2 - 0.01X_1X_3 - 0.00X_1X_4 - 0.00X_2X_3 - 0.00X_2X_4 + 0.00X_3X_4 \quad (10)$$

Table- 4 Results from CCD for CV dye biosorption by *G. pusillum*

Run no.	X_1, pH	X_2, C_o	X_3, W	X_4, T	% biosorption of CV dye	
					Experimental	Predicted
1	5	15	20	293	74.48	74.49
2	5	15	20	313	76.98	76.99
3	5	15	30	293	75.78	75.79
4	5	15	30	313	78.42	78.38
5	5	25	20	293	74.42	74.42
6	5	25	20	313	76.88	76.90
7	5	25	30	293	75.48	75.50
8	5	25	30	313	78.08	78.07
9	7	15	20	293	75.38	75.41
10	7	15	20	313	77.92	77.87
11	7	15	30	293	76.52	76.47
12	7	15	30	313	79.00	79.02
13	7	25	20	293	76.52	76.53
14	7	25	20	313	78.96	78.97
15	7	25	30	293	77.36	77.37
16	7	25	30	313	79.92	79.89
17	4	20	25	303	61.66	61.64
18	8	20	25	303	64.36	64.38
19	6	10	25	303	81.58	81.60
20	6	30	25	303	82.42	82.40
21	6	20	15	303	80.92	80.89
22	6	20	35	303	83.08	83.11
23	6	20	25	283	78.52	78.49
24	6	20	25	323	83.48	83.51

ISSN- 2394-5125 VOL 7, ISSUE 05, 2020

25	6	20	25	303	90.00	90.00
26	6	20	25	303	90.00	90.00
27	6	20	25	303	90.00	90.00
28	6	20	25	303	90.00	90.00
29	6	20	25	303	90.00	90.00
30	6	20	25	303	90.00	90.00

Test conditions [Coded Values] and watched reaction estimations of focal composite plan with 24 factorial runs, 6-main issues and 8-pivotal focuses. Fomentation time fixed at 50 min and biosorbent size at 53 μm

Table-5 speaks to the outcomes acquired in CCD. Reaction got from relapse in equation 10 as ANOVA is introduced. From the Fisher's F-test (Fmodel = 38160) and a low likelihood esteem (Pmodel>F=0.000000), it is known from table–5.5 that the model is profoundly noteworthy. At 5% level, the processed F-esteem (F0.05 (14.15) = MS model/MS error = 38160) is more prominent than that of the even F-esteem (F0.05 (14.15) tabular = 2.42), demonstrating that the treatment contrasts are critical

Table 5- ANOVA of CV dye biosorption for entire quadratic model

Source of variation	SS	Df	Mean square(MS)	F-value	*P*> F
Model	1393.064	14	99.5045	93872	0.00000
Error	0.016	15	0.00106		
Total	1393.080				

df- degree of freedom; SS- sum of squares; F- factor F; *P*- probability

R^2=0.99999; R^2 (adj):0.99998:

Table-6 estimated regression coefficients for the CV dye biosorption onto *G. pusillum*

Terms	Regression coefficient	Standard error of the coefficient	t-value	*P*-value
Mean/Intercept	-2341.18	6.208383	-377.10	0.000000
Dosage, w, g/L (L)	47.94	0.264062	307.16	0.000000
Dosage, w, g/L (Q)	-6.75	0.006243	-1080.78	0.000000
Conc, Co, mg/L (L)	1.94	0.052133	57.12	0.000000
Conc, Co, mg/L (Q)	-0.08	0.000250	-320.28	0.000000
pH (L)	0.84	0.052440	78.18	0.000000
pH (Q)	-0.08	0.000250	-320.28	0.000000
Temperature, T, K (L)	9.92.76	0.038510	357.19	0.000000
Temperature, T, K (Q)	-0.02	0.000062	-360.33	0.000000

ISSN- 2394-5125 VOL 7, ISSUE 05, 2020

1L by 2L	0.06	0.001635	36.25	0.000000
1L by 3L	-0.01	0.001635	-7.49	0.000002
1L by 4L	-0.00	0.000817	-1.38	0.188897
2L by 3L	-0.00	0.000327	-6.88	0.000005
2L by 4L	-0.00	0.000163	-0.76	0.456331
3L by 4L	0.00	0.000163	2.60	0.020104

[a] insignificant ($P \geq 0.05$)

$$\boldsymbol{Y = -2341.18 + 47.94X_1 + 1.94X_2 + 0.84X_3 + 9.92\,X_4 - 6.75X_1^2 - 0.08X_2^2 - 0.08X_3^2 - 0.02X_4^2 + 0.06X_1X_2 - 0.01X_1X_3 - 0.00\,X_1X_4 - 0.00\,X_2X_3 - 0.00\,X_2X_4 + 0.00\,X_3X_4} \quad \text{------ (11)}$$

The bigger the estimation of t and littler the estimation of P, the more critical is the comparing coefficient term. The 't' and 'P' values are broke down from table-6. It is discovered that the X1, X2, X3, X4, X12,X22, X32, X42,X1X2, X1X3, X2X3 and X2X4 have high essentialness to clarify the individual and collaboration impact of autonomous factors onCVdye biosorption. Different terms (X1X2, X1X4, X2X3,X2X4 and X3X4) are inconsequential and are not needed to clarify biosorption. A synergistic impact is shown by certain indication of the coefficient which implies reaction increments with an expansion basically, while an adversarial impact is demonstrated by a negative sign which implies reaction diminishes with an expansion as a result. In the watched reaction esteems, a proportion of the models inconstancy is given by the relationship coefficient (R2). In the current investigation, the estimation of the relapse coefficient (R2 = 0.9999) for eq.5.11indicates that 0.001 % of the allout varieties are not acceptably clarified by the model. It is demonstrated from that table that Fstatistics esteem for whole model is higher. This enormous worth implies that % biosorption can be sufficiently clarified by the model condition. For the most part P esteems lower than 0.05 demonstrates that the model is viewed as measurably huge at 95% certainty level. The % biosorption expectation from the model is appeared in table-6.

It is inferred from table-7 that all the squared terms of the apparent multitude of factors and the direct terms are noteworthy (P < 0.05). Among the cooperation terms, all the terms (P < 0.05) are inconsequential on the biosorption limit. Fig.9 and Fig.10 shows pareto outline and ordinary likelihood plot (NPP) of remaining qualities. It could be seen that the trial focuses are sensibly adjusted proposing ordinary appropriation.

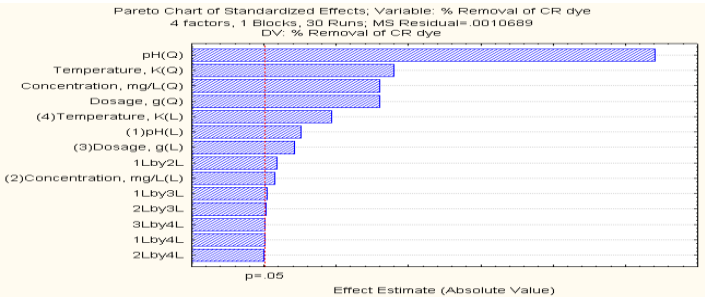

Fig.-9 Pareto Chart

ISSN- 2394-5125 VOL 7, ISSUE 05, 2020

The ideal arrangement of conditions for greatest rate biosorption of CV dye is pH = 6.0502, introductory CV dye focus = 20.2557 mg/L, biosorbent dose = 25.6967 g/L, and temperature = 305.8028 K. The degree of biosorption of CV dye at these ideal conditions was 90.23709 %. It is apparent that exploratory estimations of % biosorption are in close concurrence with that of anticipated by Central Composite Design. Analyses are directed in triplicate with the above anticipated ideal arrangement of conditions and the % biosorption of CV dye is 93 %, which is nearer to the anticipated % biosorption.

7.2. Interaction effects of biosorption variables

The three-dimensional perspective on reaction surface shape plots [Fig. 11 (a) to (f)] show % biosorption as an element of for different mixes of autonomous factors. The plots are spoken to as a component of two factors one after another keeping different elements fixed at zero level.

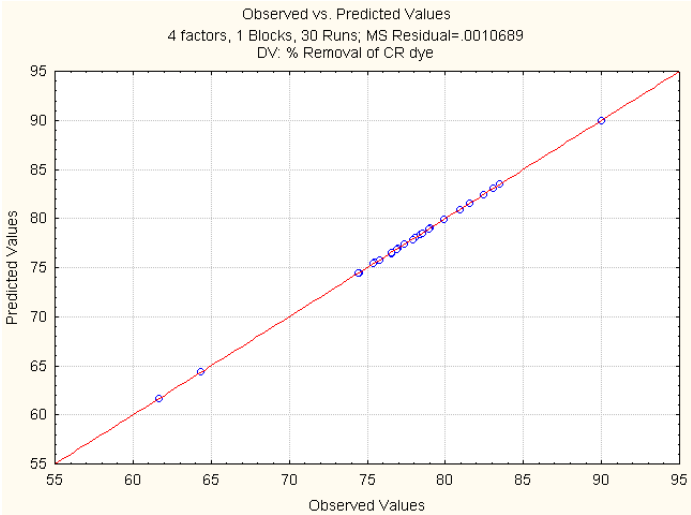

Fig. 10 Normal probability plot for % biosorption of CV dye

It is found from the reaction surface plots that the % biosorption is maximal at low and elevated levels of the info factors. Notwithstanding, there exists a district where neither an expanding nor a diminishing pattern in % biosorption is watched. The biosorption factors ought to be ideal to boost the % biosorption. The % biosorption of CV dye is firmly affected by the pH as clear from figs. 5.15 (a)& (b).

The anticipated ideal arrangement of conditions for rate biosorption of CV dye is

pH	=	6.0502
Initial CV dye concentration	=	20.2557 mg/L
Biosorbent dosage	=	25.6967 g/L
Temperature	=	305.6967 K
% biosorption of CV dye	=	90.23709

The ideal arrangement of conditions acquired with CCD is appeared in table-5.7 alongside trial esteems.

ISSN- 2394-5125 VOL 7, ISSUE 05, 2020

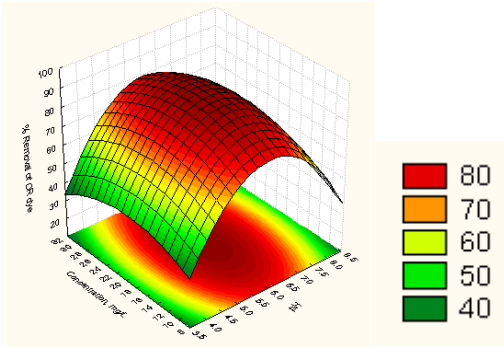

Fig. 11 (a) Surface contour plot for the effects of pH and initial CV dye concentration on % biosorption

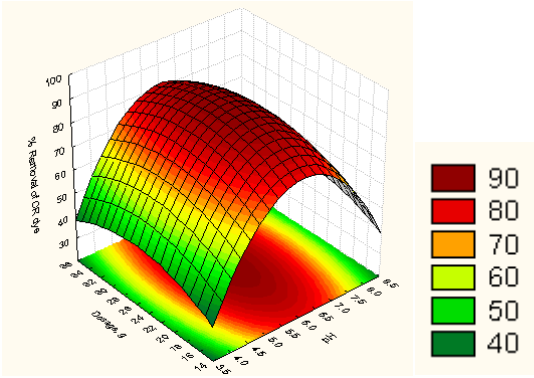

Fig. 11 (b) Surface contour plot for the effects of pH and dosage on % biosorption of CV dye

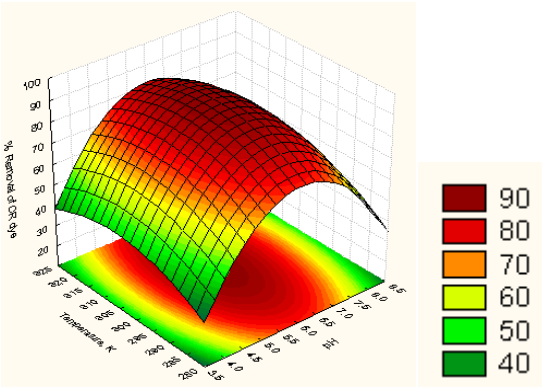

Fig.11 (c) Surface contour plot for the effects of pH and Temperature on % biosorption of CV dye

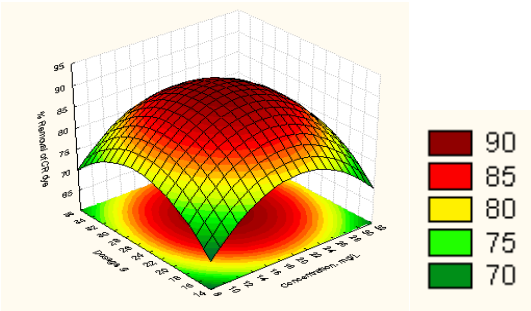

Fig. 11 (d) Surface contour plot for the effects of initial concentration and dosage on % biosorption of CV dye

ISSN- 2394-5125 VOL 7, ISSUE 05, 2020

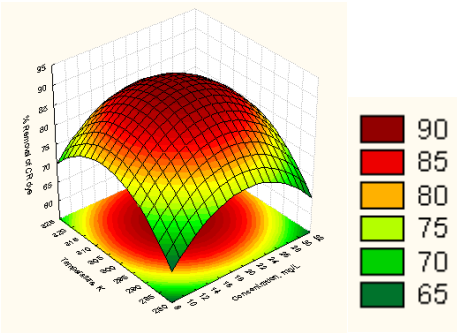

Fig. 11 (e) Surface contour plot for the effects of initial concentration and Temperature on % biosorption of CV dye

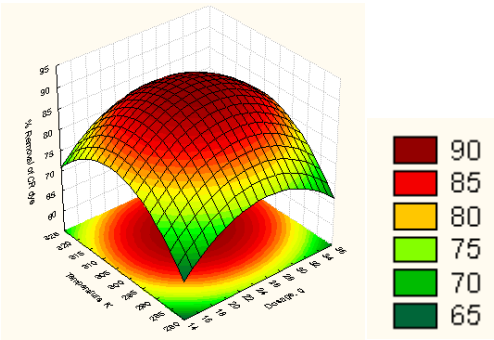

Fig. 11 (f) Surface contour plot for the effects of Dosage and Temperature on % biosorption of CV dye

Table 7 Comparison between optimum values from CCD and experimentation

Variable	CCD	Experimental value
pH of aqueous solution	6.0502	6
Initial cobalt concentration, mg/L	20.2557	20
Biosorption dosage, w, g/L	25.6967	25
Temperature, K	305.8028	303
% biosorption	90.23709	95.0

8. Conclusion

The maximum sorption of CV dye (90.23709 %) onto *G. pusillum* is observed when the processing parameters are set as: pH = 6.0245, w = 25.6967 g/L, Co = 20.2557 mg/L and T = 305.8028 K using CCD. The thermodynamic data show that % sorption of CV dye is increased with increase in temperature. The investigation also reveals the endothermic nature of sorption as ΔH is positive (14.7433 J/mole), irreversible nature of sorption as ΔS is positive (13.0993 J/mole.K) and spontaneity of sorption as indicated by negative ΔG (–1105.35 J/mole).

Acknowledgements

We are thankful to the Prof. P. J. Rao Department of Chemical Engineering for designing, execution and writing of proposed research work and I extended my deepest gratitude to Dr. Ch. Asha Immanuel Raju for helping in analysis and characterization of samples.

Conflict of Interest The authors declare no competing interests.

Reference

1. Grace Pavithra, K, Senthil Kumar P., Jaikumar V., Sundar Rajan P. Removal of colorants from wastewater: A review on sources and treatment strategies. Journal of Industrial and Engineering Chemistry, 2019; 75; 1-19.
2. Abate Ayele, Deribe Getachew, M. Kamaraj, A. Suresh, "Phycoremediation of Synthetic Dyes: An Effective and Eco-Friendly Algal Technology for the Dye Abatement", Journal of Chemistry, 2021, 14 pages, 2021.
3. Smriti R, Dimitrios K, Brajesh S, Emerging technologies in bioremediation: Constraints and opportunities, Biodegradation 2012; 23(6):917-26.
4. Vanitha K, Jibrail K, Sie Yon L, Efficiency of various recent wastewater dye removal methods: A review, Journal of Environmental Chemical Engineering,2018; 6 (4); 4676-4697.
5. Mouni Roy, Rajnarayan Saha, Dyes and their removal technologies from wastewater: A critical review, Intelligent Environmental Data Monitoring for Pollution Management, 2021; 6; 127-160.
6. Dogan, M. and Alkan, M.,"Removal of methyl violet from aqueous solutions by perlite", J. Colloid Interface Sci.,2003; 267; 32-41.
7. Sukhada Saraf and Varsha, K. Vaidya.. "Comparative Study of Biosorption of Textile Dyes Using Fungal Biosorbents", Int. J. Curr. Microbiol. App. Sci, 2015; 357-365.
8. T. Suganya, M. Varman, H.H. Masjuki, S. Renganathan. Macroalgae and microalgae as a potential source for commercial applications along with biofuels production: A biorefinery approach, Renewable and Sustainable Energy Reviews, 2016; 55; 909-941.
9. Hemant Mittal, Ali Al Alili, Saeed M. Alhassan. Adsorption isotherm and kinetics of water vapors on novel superporous hydrogel composites, Microporous and Mesoporous Materials, 2020; 299;110106.
10. Michalak I, Chojnacka K, Witek-Krowiak A. State of the art for the biosorption process--a review. Appl Biochem Biotechnol. 2013; 170(6); 1389-416.
11. Xiaodong Yang, Lili Wang, Xueqin Shao, Jin Tong, Rui Chen, Qiang Yang, Xizhen Yang, Guodong Li, Andrew R. Zimmerman, Bin Gao, Preparation of biosorbent for the removal of organic dyes from aqueous solution via one-step alkaline ball milling of hickory wood, Bioresource Technology, 2022, 126831.
12. Santos, F.A., Alban, L., Frankenberg, C.L.C. Pires M. International Journal of Environmental Science and Technology Characterization and use of biosorbents prepared from forestry waste and their washed extracts to reduce/remove chromium. Int. J. Environ. Sci. Technol, 2016; 13, 327–338.
13. Farooqa M.U, Jalees, M.I. Iqbala, A, Zahraa, N, Kirana, A. Desalination and water tre atment science and engineering, Characterization and adsorption study of biosorbents for the removal of basic cationic dye: kinetic and isotherm analysis. 2019; 160333–342.

14. Stavrinou, A., Aggelopoulos, C. A., & Tsakiroglou, C. D. "Exploring the adsorption mechanisms of cationic and anionic dyes onto agricultural waste peels of banana, cucumber, and potato: adsorption kinetics and equilibrium isotherms as a tool". Journal of environmental chemical engineering, 2018); 6(6), 6958-6970.
15. Pahalagedara, M. N., Samaraweera, M., Dharmarathna, S., Kuo, C. H., Pahalagedara, L. R., Gascón, J. A., & Suib, S. L. "Removal of azo dyes: intercalation into sonochemically synthesized NiAl layered double hydroxide". *The Journal of Physical Chemistry C*, 2014; 118(31), 17801-17809.
16. Kausar, A., Naeem, K., Hussain, T., Bhatti, H. N., Jubeen, F., Nazir, A., & Iqbal, M. "Preparation and characterization of chitosan/clay composite for direct Rose FRN dye removal from aqueous media: comparison of linear and non-linear regression methods". *Journal of Materials Research and Technology*, 2019; *8*(1), 1161-1174.
17. Wang, L., Zhang, J., Zhao, R., Li, C., Li, Y., & Zhang, C. "Adsorption of basic dyes on activated carbon prepared from Polygonum orientale Linn: equilibrium, kinetic and thermodynamic studies". *Desalination*, 2010; 254(1-3), 68-74.
18. Janoš, P., Michálek, P., & Turek, L. "Sorption of ionic dyes onto untreated low-rank coal–oxihumolite: A kinetic study". *Dyes and Pigments*, 2007; 74(2), 363-370.
19. Kallel, F., Bouaziz, F., Chaari, F., Belghith, L., Ghorbel, R., & Chaabouni, S. E. "Interactive effect of garlic straw on the sorption and desorption of Direct Red 80 from aqueous solution". *Process Safety and Environmental Protection*, 2016; 102, 30-43.
20. Kyzas, G. Z., & Lazaridis, N. K. "Reactive and basic dyes removal by sorption onto chitosan derivatives". *Journal of Colloid and Interface Science*, 2009; 331(1), 32-39.
21. Souza-Silva, Érica A., Emanuela Gionfriddo, Md Nazmul Alam, Janusz Pawliszyn. Insights into the effect of the PDMS-layer on the kinetics and thermodynamics of analyte sorption onto the matrix-compatible solid phase microextraction coating". *Analytical chemistry*, 2017 "89(5), 2978-2985.
22. Aviara, N. A., O. O. Ajibola, S. A. Oni.."Sorption equilibrium and thermodynamic characteristics of soya bean". *Biosystems Engineering*, 2004; 87(2), 179-190.
23. Igwegbe, C. A., Mohmmadi, L., Ahmadi, S., Rahdar, A., Khadkhodaiy, D., Dehghani, R., & Rahdar, S. "Modeling of adsorption of methylene blue dye on Ho-CaWO4 nanoparticles using response surface methodology (RSM) and artificial neural network (ANN) techniques". Methods 2019; 6; 1779-1797.
24. Singh, K. P., Gupta, S., Singh, A. K., & Sinha, S. "Optimizing adsorption of crystal violet dye from water by magnetic nanocomposite using response surface modeling approach". *Journal of hazardous materials*, 2011; 186(2-3), 1462-1473